PAPER

NJC
www.rsc.org/njc

Syntheses, crystal structures and anion-exchange properties of copper(II) and cadmium(II) complexes containing a novel tripodal ligand†

Wei Zhao,[a] Jian Fan,[a] Taka-aki Okamura,[b] Wei-Yin Sun*[a] and Norikazu Ueyama[b]

[a] *Coordination Chemistry Institute, State Key Laboratory of Coordination Chemistry, Nanjing University, Nanjing 210093, P. R. China. E-mail: sunwy@nju.edu.cn*
[b] *Department of Macromolecular Science, Graduate School of Science, Osaka University, Toyonaka, Osaka, 560-0043, Japan*

Received (in Montpellier, France) 29th December 2003, Accepted 7th April 2004
First published as an Advance Article on the web 20th July 2004

Four novel metal-organic frameworks (MOFs), $[Cu(\mathbf{3})_2](ClO_4)_2\cdot 0.67H_2O$ (**4**), $[Cu(\mathbf{3})_2][Cu(mal)_2]\cdot 6H_2O$ ($mal^{2-} = {}^{-}OCOCH_2COO^{-}$) (**5**), $[Cd(\mathbf{3})_2](NO_3)_2\cdot H_2O$, (**6**) and $[Cd(\mathbf{3})(OAc)_2]\cdot 6H_2O$ (**7**), were obtained by self-assembly of the corresponding metal salts with a novel flexible tripodal ligand, 1-(1-imidazolyl)-3,5-bis(imidazol-1-ylmethyl)benzene (**3**), and their structures were determined by single crystal X-ray diffraction analyses. Complex **4** has a 2D network structure in which **3** shows two different coordination modes, one kind of **3** acts as a three-connecting ligand and the other one serves as a two-connecting (bridging) ligand using its two flexible arms. Complex **5** has an infinite 1D hinged chain structure in which only two of three imidazole groups of **3** are coordinated with the metal atoms while the last one is uncoordinated. In complexes **6** and **7**, the metal centers are all six-coordinated; **6** has a 2D honeycomb and **7** has a 2D grid network structure, respectively. Ligand **3** has a trans conformation in **7**, which is different from that in complexes **4** (cis and L-shaped), **5** (cis) and **6** (cis). The anion-exchange properties of complex **6** were investigated.

Introduction

In the past decade, much progress has been achieved in the metal-directed assembly of supramolecular frameworks with suitable metal ions and rationally designed organic ligands.[1] Metal-organic frameworks (MOFs) with specific topologies such as cage-like structures, honeycomb and interpenetrating networks have been obtained by self-assembly of suitable metal salts with rigid or flexible tripodal ligands, for example, 1,3,5-tricyanobenzene,[2] 2,4,6-tris(4-pyridyl)-1,3,5-triazine,[3] 1,3,5-benzenetribenzoate,[4] 1,3,5-tris(4-pyridylmethyl)benzene[5] and 1,3,5-tris(benzimidazole-1-ylmethyl)-2,4,6-trimethylbenzene.[6] In contrast to the rigid ligands that show little or no conformational changes when they interact with metal salts, the flexible tripodal ligands have many more possible coordination modes due to their flexibility and they can adopt different conformations according to the geometric requirements of different metal ions. Accordingly, we designed and synthesized a series of flexible tripodal ligands with aromatic core as spacers and systematically investigated their reactions with metal salts.[7]

Most recently, interest in porous metal-organic frameworks has been driven by the prospect of generating a wide range of materials with useful properties for applications such as adsorption, ion and molecular recognition, ion-exchange and catalysis.[8–10] Supramolecular architectures have attracted much attention not only because of their various structures, but also because of their potential applications.[11–15] Yaghi and co-workers have reported MOFs containing large rectangular channels obtained by self-assembly of $Cu(NO_3)_2\cdot 2.5H_2O$ with 4,4′-bipyridine.[11a] In this complex, most of the nitrate ions can be exchanged by SO_4^{2-} and BF_4^{-}.[11a] Yip and co-workers have also reported the anion exchange of coordination polymers with silver(I) and flexible ligands.[11b]

In our previous studies, we reported two tripodal ligands, 1,3,5-tris(1-imidazolyl)benzene (**1**, Scheme 1) and 1,3-bis(1-imidazolyl)-5-(imidazol-1-ylmethyl)benzene (**2**, Scheme 1) and demonstrated that they can form organic-inorganic hybridized coordination complexes with reversible anion-exchange properties.[12] The results show that such tripodal ligands are versatile and can adopt different conformations when they interact with metal salts and the self-assembly process depends on many and/or even subtle factors and is often difficult to predict exactly.[13] This encouraged us to undertake further studies on analogs/derivatives of **1** and **2** as organic ligands, which may lead to a great variety of structures. Following this approach, we now expand this system with a new tripodal ligand, 1-(1-imidazolyl)-3,5-bis(imidazol-1-ylmethyl)benzene (**3**, Scheme 1). Four non-interpenetrating organic-inorganic hybridized coordination complexes, $[Cu(\mathbf{3})_2](ClO_4)_2\cdot 0.67H_2O$ (**4**), $[Cu(\mathbf{3})_2][Cu(mal)_2]\cdot 6H_2O$ (**5**), $[Cd(\mathbf{3})_2](NO_3)_2\cdot H_2O$ (**6**) and $[Cd(\mathbf{3})(OAc)_2]\cdot 6H_2O$ (**7**), were successfully isolated; their structures and the anion-exchange behavior of complex **6** were investigated.

Experimental

Materials and methods

All commercially available chemicals were of reagent grade and were used as received without further purification. Solvents were purified according to the standard methods. C, H and N analyses were made on a Perkin–Elmer 240C elemental analyzer at the analysis center of Nanjing University. ^{1}H NMR spectral measurements were performed on a Bruker DRX-500

† Electronic supplementary information (ESI) available: crystal packing diagrams and hydrogen bonding for **4**–**7**; XPD of **6** and its ion-exchanged analogs. See http://www.rsc.org/suppdata/nj/b3/b317043h/

DOI: 10.1039/b317043h

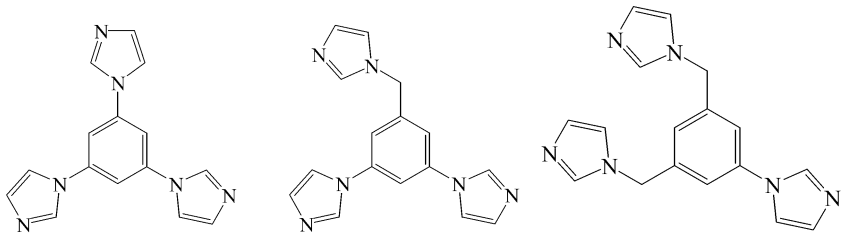

1 2 3

Scheme 1

NMR spectrometer at room temperature. Infrared (IR) spectra were recorded on a Bruker Vector22 FT-IR spectrophotometer by using KBr discs. Powder X-ray diffraction patterns were taken on a Rigaku D/max-RA rotating anode X-ray diffractometer with graphite-monochromated Cu-Kα ($\lambda = 1.542$ Å) radiation at room temperature. Thermogravimetric and differential thermal analyses were performed on a simultaneous SDT 2960 thermal analyzer. Powder samples were loaded into alumina pans and heated under N_2at a heating rate of 10 °C min^{-1}.

Syntheses

1-(1-Imidazolyl)-3,5-bis(imidazol-1-ylmethyl)benzene (3). 1-Bromo-3,5-dimethylbenzene was treated with *N*-bromosuccinimide to give 1-bromo-3,5-bis(bromomethyl)benzene, which was then treated with imidazole in DMSO to generate 1-bromo-3,5-bis(imidazole-1-ylmethyl)benzene. 1-Bromo-3,5-bis(imidazole-1-ylmethyl)benzene (2.52 g, 8.0 mmol), imidazole (1.63 g, 24.0 mmol), K_2CO_3 (1.46 g, 10.4 mmol), and $CuSO_4$ (0.05 g, 0.20 mmol) were mixed and heated at 180 °C for 12 h under a nitrogen atmosphere. The mixture was cooled to room temperature and was then washed with water. The residue was extracted with CH_2Cl_2 (5×30 ml). The organic layer was separated, dried over sodium sulfate and evaporated to dryness to give the crude product **3**, which was recrystallized from water and methanol. Yield: 40%. ^{1}H NMR [$CDCl_3$] δ: 7.79 (s, 1H), 7.61 (s, 2H), 7.22 (s, 1H), 7.19 (s, 1H), 7.17 (s, 2H), 7.10 (s, 2H), 6.93 (s, 2H), 6.89 (s, 1H), 5.19 (s, 4H). Elem. anal. for **3**, $C_{17}H_{16}N_6$: C, 66.90; H, 5.65; N, 27.45%; calcd: C, 67.09; H, 5.30; N, 27.61%.

$[Cu(3)_2](ClO_4)_2 \cdot 0.67H_2O$ (4). The title compound was synthesized by a hydrothermal reaction. A mixture of 0.5 mmol (21.7 mg) of [Cu(dien)im]$(ClO_4)_2$(dien = $NH_2CH_2CH_2NHCH_2CH_2NH_2$; im = imidazole), 0.5 mmol (15.2 mg) of **3** and 10.0 ml of deionized water was sealed into a bomb equipped with a Teflon liner and then heated at 100 °C for 4 days. After slow cooling of the reaction mixture to room temperature, blue crystals of compound **4** were obtained in *ca.* 62% yield as a single phase. Anal. calcd for $C_{34}H_{33.13}Cl_2CuN_{12}O_{8.67}$: C, 46.25; H, 3.78; N, 19.04%. Found: C, 46.10; H, 3.66; N, 18.85%. IR (KBr, cm^{-1}): 3386 m, 3133 m, 1610 m, 1524 m, 1442 m, 1237 m, 1094 s, 948 m, 828 m, 754 m, 739 m, 659 m, 622 m. The TGA data of **4** show an initial weight loss of 1.5% (calcd. 1.4%) from 30 to 100 °C, representing the loss of 0.67 uncoordinated water molecules.

Caution! Perchlorate salts of metal complexes with organic ligands are potentially explosive and should be handled with care.

$[Cu(3)_2][Cu(mal)_2] \cdot 6H_2O$ ($mal^{2-} = {}^{-}OCOCH_2COO^{-}$) (5). An aqueous solution (10 ml) of CuO (4.0 mg, 0.05 mmol) and H_2mal (5.2 mg, 0.05 mmol) was refluxed and stirred for about 8 h. The aqueous solution was filtered and cooled down to room temperature. A blue powder was obtained after mixing the aqueous solution and **3** (15.2 mg, 0.05 mmol) in methanol (2.5 ml) at room temperature. Yield: 47%. Single crystals suitable for X-ray analysis were obtained by recrystallization from a mixed solution of H_2O (5 ml) and acetonitrile (5 ml) at room temperature for 7 days. Anal. calcd for $C_{40}H_{48}Cu_2N_{12}O_{14}$: C, 45.84; H, 4.62; N, 16.04%. Found: C, 45.88; H, 4.66; N, 16.03%. IR (KBr, cm^{-1}): 3385 s, 3133 m, 1605 s, 1605 s, 1561 s, 1531 m, 1501, 1420 m, 1400 m, 1371 m, 1316 m, 1245 m, 1233 m, 1094 m, 1060 m, 835 m, 749 m, 737 m, 686 m, 664 m, 635 m. The TGA data of **5** show an initial weight loss of 10.1% (calcd. 10.3%) from 30 to 80 °C, representing the loss of uncoordinated water molecules; no further weight loss was observed over the temperature range 80–175 °C.

$[Cd(3)_2](NO_3)_2 \cdot H_2O$ (6). This complex was prepared by slow diffusion between two layers of an aqueous solution (10 ml) of $Cd(NO_3)_2 \cdot 4H_2O$ (15.4 mg, 0.05 mmol) and **3** (15.2 mg, 0.05 mmol) in methanol (10 ml) at room temperature. About two weeks later, colorless platelet crystals suitable for X-ray analysis were obtained in 50% yield. Anal. calcd for $C_{34}H_{34}CdN_{14}O_7$: C, 47.31; H, 3.97; N, 22.72%. Found: C, 47.32; H, 3.94; N, 22.68%. IR (KBr, cm^{-1}): 3446 m, 3121 m, 1609 m, 1510 m, 1439 m, 1384 s, 1336 m, 1231 m, 1108 m, 1086 m, 1069 m, 1035 m, 933 m, 830 m, 738 m, 660 m, 634 m. The TGA data of **6** show an initial weight loss of 2.0% (calcd. 2.1%) from 20 to 100 °C, representing the loss of uncoordinated water molecules; no further weight loss was observed over the temperature range 100–320 °C.

$[Cd(3)(OAc)_2] \cdot 6H_2O$ (7). In a typical synthesis, an aqueous solution (5 ml) of $Cd(OAc)_2 \cdot 2H_2O$ (13.3 mg, 0.05 mmol) was added slowly to a solution of **3** (15.2 mg, 0.05 mmol) in H_2O (5 ml) and the mixture was stirred for 5 h at room temperature to give a colorless powder in *ca.* 80% yield. Single crystals suitable for X-ray analysis were obtained by recrystallization from methanol solution. Anal. calcd for $C_{21}H_{34}CdN_6O_{10}$: C, 39.23; H, 5.33; N, 13.07%. Found: C, 39.42; H, 5.44; N, 13.07%. IR (KBr, cm^{-1}): 3405 s, 3125 m, 1607 m, 1563 s, 1508 s, 1437 m, 1415 m, 1437 m, 1415 m, 1314 m, 1227 m, 1109 m, 1092 m, 1069 m, 1015 m, 935 m, 838 m, 748 m, 660 m, 620 m. The TGA data of **7** show an initial weight loss of 16.5% (calcd. 16.8%) from 20 to 110 °C, representing the loss of uncoordinated water molecules; no further weight loss was observed over the temperature range 110–300 °C.

Anion-exchange reactions

Well-ground powder of $[Cd(3)_2](NO_3)_2 \cdot H_2O$ (**6**, 200.0 mg) was suspended in water (20 mL), then $NaClO_4$ (1.5 g) was added. The mixture was stirred for 1 day at room temperature, then filtered, washed with water several times and dried. Elem. anal. for the exchanged powder: C, 43.48; H, 3.61; N, 17.80%; calcd for $[Cd(3)_2](ClO_4)_2 \cdot H_2O$: C, 43.54; H, 3.65; N, 17.92%. The exchanged solid (200.0 mg) was suspended in water (20 mL) and $NaNO_3$ (1.5 g) was added. The mixture was stirred for

Table 1 Crystallographic data for complexes **4**, **5**, **6** and **7**

Compound	**4**	**5**	**6**	**7**
Chemical formula	$C_{34}H_{33.13}Cl_2CuN_{12}O_{8.67}$	$C_{40}H_{48}Cu_2N_{12}O_{14}$	$C_{34}H_{34}CdN_{14}O_7$	$C_{21}H_{34}CdN_6O_{10}$
M	883.27	1047.98	863.15	642.94
Crystal system	Monoclinic	Triclinic	Triclinic	Triclinic
Space group	$P2_1/c$	P-1	P-1	P-1
Z	4	1	2	2
a/Å	19.693(9)	8.860(6)	12.301(13)	11.2414(6)
b/Å	8.996(5)	10.518(7)	12.992(17)	12.1178(2)
c/Å	20.591(8)	12.331(8)	13.221(14)	12.2494(6)
α/°	90.00	81.71(5)	70.85(9)	60.400(2)
β/°	97.57(3)	76.18(5)	66.48(8)	77.0554(16)
γ/°	90.00	82.76(5)	78.79(8)	70.382(3)
T/K	200	200	200	200
U/Å^3	3616(3)	1099.2(12)	1825(4)	1363.20(10)
μ/mm^{-1}	0.826	1.050	0.668	0.863
Data collected	35 596	10 942	17 657	12 953
Independent data	8229	5010	8221	6172
R_{int}	0.1873	0.0558	0.1054	0.0284
Observed data	3274	3419	2532	5613
R_1 [$I > 2\sigma(I)$]	0.0560	0.0379	0.0472	0.0266
wR_2 [$I > 2\sigma(I)$]	0.0885[a]	0.0766[b]	0.0659[c]	0.0686[d]
R_1 (all data)	0.1579	0.0625	0.1558	0.0311
wR_2 (all data)	0.1080	0.0803	0.0744	0.0702

[a] $w = 1/[\sigma^2(F_0)^2]$. [b] $w = 1/[\sigma^2(F_0)^2 + (0.0359P)^2]$, $P = (F_0^2 + 2F_c^2)/3$. [c] $w = 1/[\sigma^2(F_0)^2]$. [d] $w = 1/[\sigma^2(F_0)^2 + (0.0428P)^2 + 0.4550P]$, $P = (F_0^2 + 2F_c^2)/3$.

1 day at room temperature, then filtered, washed with water several times and dried to give a colorless powder. Elem. anal. for this powder: C, 45.58; H, 3.89; N, 20.17%; calcd for $[Cd(\mathbf{3})_2](ClO_4)(NO_3)\cdot H_2O$: C, 45.30; H, 3.78; N, 20.21%.

Well-ground powder of $[Cd(\mathbf{3})_2](NO_3)_2\cdot H_2O$ (**6**, 200.0 mg) was suspended in water (20 mL), then $NaNO_2$ (1.5 g) was added. The mixture was stirred for 1 day at room temperature, then filtered, washed with water several times and dried. Elem. anal. for the exchanged product: C, 49.20; H, 4.18; N, 23.55%; calcd for $[Cd(\mathbf{3})_2](NO_2)_2\cdot H_2O$: C, 49.13; H, 4.12; N, 23.59%. The exchanged solid (200.0 mg) was suspended in water (20 mL) and $NaNO_3$ (1.5 g) was added. The mixture was stirred for 1 day at room temperature, then filtered, washed with water several times, and dried to give a colorless powder. Elem. anal. for the exchanged powder: C, 47.35; H, 3.95; N, 22.70%; calcd for $[Cd(\mathbf{3})_2](NO_3)_2\cdot H_2O$: C, 47.31; H, 3.97; N, 22.72%.

X-Ray crystallography

The collection of crystallographic data for the complexes **4**, **5**, **6** and **7** was carried out on a Rigaku RAXIS-RAPID Imaging Plate diffractometer at 200 K, using graphite-monochromated Mo-Kα radiation ($\lambda = 0.7107$ Å). The structures were solved by direct methods with SIR92[16] and expanded using Fourier techniques.[17] All non-hydrogen atoms were refined anisotropically by the full-matrix least-squares method. The hydrogen atoms except for those of water molecules were generated geometrically. In complex **4**, eight oxygen atoms of two perchlorate anions are disordered into two positions with site occupancy factors (SOF) of 0.734(5) for O1, O2, O3, O4, 0.266(5) for O1B, O2B, O3B, O4B, 0.810(10) for O5, O6, O7, O8 and 0.190(10) for O5B, O6B, O7B, O8B. All calculations were carried out on an SGI work station using the teXsan crystallographic software package of Molecular Structure Corporation.[18] Details of the crystal parameters, data collection and refinement are summarized in Table 1; selected bond lengths and angles with their estimated standard deviations are listed in Table 2.‡

‡ CCDC reference numbers 236959–236962. See http://www.rsc.org/suppdata/nj/b3/b317043h/ for crystallographic data in .cif or other electronic format.

Results

Crystal structures

$[Cu(\mathbf{3})_2](ClO_4)_2\cdot 0.67H_2O$ (4). The title complex crystallizes in the monoclinic form with space group $P2_1/c$. As shown in Fig. 1, each copper(II) atom in complex **4** is coordinated by five N atoms from five different **3** ligands. Due to the presence of two flexible arms, ligand **3** can coordinate to the metal center comfortably to meet the geometric requirements of Cu(II). The coordination geometry of the Cu(II) center can be described as a tetragonal pyramid with an N_5 donor set. The Cu–N bonds in the equatorial plane have very similar bond lengths ranging from 1.983(4) to 1.997(4) Å, while the ligand at the apical position shows an elongated bond length of Cu1–N52 = 2.253(4) Å. The N–Cu–N coordination angles range from 87.27(15) to 173.92(17)° (Table 2). The Cu1 atom locates approximately within the plane formed by the N12, N32, N132 and N152 atoms with a deviation of 0.20 Å. It is interesting that there are two kinds of ligands **3** with different conformations. Ligand **3A** has a cis conformation since the two coordinating atoms N52A and N32A from the two flexible arms locate above the central benzene ring plane with distances of 3.13 and 2.13 Å, respectively. In the case of ligand **3B**, the atom N15B locates above the central benzene ring plane at a distance of 2.32 Å and the corresponding distance between N132 and the central benzene ring plane is only 0.27 Å. This means that ligand **3B** has a near-L shape (Scheme 2), rather than the cis or trans conformation, in complex **4**. For ligand **3A**, the three imidazolyl rings are inclined to the phenyl ring with angles of 77.1°, 93.4° and 107.7° and the corresponding angles are 43.6°, 85.6°, 89.7° for ligand **3B**. Neglecting the interactions with ligand **3B**, three copper(II) atoms are linked by ligand **3A** to form a triangle with metal-metal separations (Cu···Cu) of 9.00, 10.59 and 12.18 Å, respectively; therefore ligand **3A** acted as a three-connecting ligand. Such units repeat in the *ab* plane to generate an infinite 2D honeycomb network as shown in Fig. 2(a). In addition, two such 2D networks are further linked by ligand **3B** bridges to form an independent layer [Fig. 2(b)]; the copper atoms between two sublayers bridged by ligand **3B** have a Cu···Cu separation of 10.89 Å. It is noteworthy that ligand **3B** has only two flexible imidazole groups coordinated with the metal atoms while the rigid one

Table 2 Selected bond distances (Å) and angles (°) for compounds **4**, **5**, **6** and **7**

Compound **4**			
Cu1–N132	1.983(4)	Cu1–N12	1.983(4)
Cu1–N32	1.985(4)	Cu1–N152	1.997(4)
Cu1–N52	2.253(4)	N132–Cu1–N12	173.92(17)
N132–Cu1–N32	91.59(15)	N12–Cu1–N32	91.82(15)
N132–Cu1–N152	87.89(15)	N12–Cu1–N152	87.27(15)
N32–Cu1–N152	161.28(16)	N132–Cu1–N52	93.35(15)
N12–Cu1–N52	91.16(15)	N32–Cu1–N52	97.99(15)
N152–Cu1–N52	100.72(15)		
Compound **5**			
Cu1–N52^a	2.019(2)	Cu1–N52	2.019(2)
Cu1–N32	2.025(2)	Cu1–N32^a	2.025(2)
Cu2–O3	1.912(2)	Cu2–O3^b	1.912(2)
Cu2–O1^b	1.927(2)	Cu2–O1	1.927(2)
N52^a–Cu1–N52	180.0	N52^a–Cu1–N32	87.61(9)
N52–Cu1–N32	92.39(9)	N52^a–Cu1–N32^a	92.39(9)
N52–Cu1–N32^a	87.61(9)	N32–Cu1–N32^a	180.0
O3–Cu2–O3^b	180.0	O3–Cu2–O1^b	85.48(9)
O3^b–Cu2–O1^b	94.52(9)	O3–Cu2–O1	94.52(9)
O3^b–Cu2–O1	85.48(9)	O1^b–Cu2–O1	180.0
Compound **6**			
Cd1–N132	2.298(5)	Cd1–N152	2.319(5)
Cd1–N52	2.326(5)	Cd1–N32	2.334(5)
Cd1–N112	2.379(5)	Cd1–N12	2.377(5)
N132–Cd1–N152	89.42(18)	N132–Cd1–N52	86.94(19)
N152–Cd1–N52	173.51(17)	N132–Cd1–N32	177.40(19)
N152–Cd1–N32	89.15(18)	N52–Cd1–N32	94.69(18)
N132–Cd1–N112	94.08(19)	N152–Cd1–N112	91.02(17)
N52–Cd1–N112	83.89(17)	N32–Cd1–N112	88.1(2)
N132–Cd1–N12	86.73(19)	N152–Cd1–N12	87.56(17)
N52–Cd1–N12	97.59(18)	N32–Cd1–N12	91.0(2)
N112–Cd1–N12	178.36(17)		
Compound **7**			
Cd1–N52	2.278(2)	Cd1–N32	2.300(2)
Cd1–O72	2.302(2)	Cd1–N12	2.320(2)
Cd1–O81	2.394(2)	Cd1–O82	2.500(2)
N52–Cd1–N32	169.61(6)	N52–Cd1–O72	88.19(6)
N32–Cd1–O72	84.89(6)	N52–Cd1–N12	90.39(6)
N32–Cd1–N12	88.45(6)	O72–Cd1–N12	131.72(6)
N52–Cd1–O81	102.49(6)	N32–Cd1–O81	87.64(6)
O72–Cd1–O81	143.58(6)	N12–Cd1–O81	83.49(6)
N52–Cd1–O82	81.00(6)	N32–Cd1–O82	107.40(6)
O72–Cd1–O82	96.04(5)	N12–Cd1–O82	131.31(6)
O81–Cd1–O82	52.71(5)		

^{a} Symmetry transformation: $-x$, $2-y$, $-z$. ^{b} Symmetry transformation: $1-x$, $1-y$, $1-z$.

keeps free of coordination; thus, this ligand served as a two-connecting (bridging) ligand, without a dimensionality increase. In short, each independent 2D layer in complex **4** contains two sublayers, which are connected by ligand **3B** bridges. Disordered perchlorate anions are located between the two sublayers of an independent layer (Fig. 3) and held there by C–H···O (ClO_4^-) hydrogen bonds to produce a 3D framework as exhibited in Figs. S1 and S5 (see Electronic supplementary information); the distances of C···O are in the range of 3.031(8)–3.478(7) Å and the C–H–O angles are in the range from 124° to 159°.[19] The hydrogen-bonding data are summarized in Table S1 (see ESI). The distances of 2.77 and 2.80 Å between the O atom of solvated water and the O atom of perchlorate or the N atom of the imidazole indicate the presence of the O–H···O and O–H···N hydrogen bonds, respectively, although the hydrogen atoms of the water molecule could not be found.

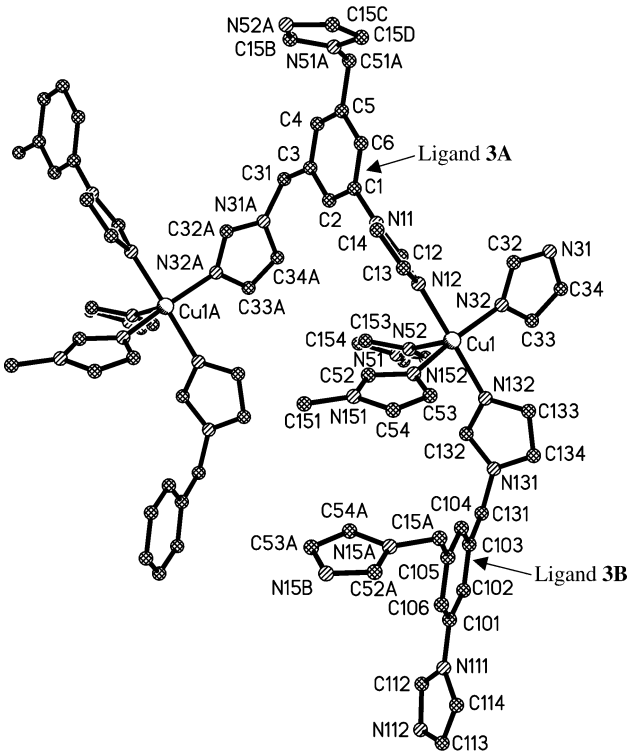

Fig. 1 Coordination environment around the copper(II) atom in **4** with the perchlorate anions, lattice water molecules and hydrogen atoms omitted for clarity.

$[Cu(3)_2][Cu(mal)_2]\cdot 6H_2O$ (5). The title complex crystallizes in the triclinic form with *P*-1 space group; the coordination environment around the copper(II) center in complex **5** is shown in Fig. 4(a). The asymmetric unit of **5** contains two distinct Cu centers, in which Cu1 and Cu2 sit on inversion centers [Fig. 4(a)]. Each Cu1 center coordinates to four N atoms from different **3** ligands with N–Cu–N bond angles in the range of 87.61(9)–180.0° and Cu–N bond distances of 2.019(2) and 2.025(2) Å. The Cu1 atom locates within the plane defined by N32, N32A, N52 and N52A atoms without deviation. Therefore, the local coordination geometry around Cu1 can be regarded as square-planar with an N_4 donor set, which is different from that in **4**. Each ligand **3** in turn binds to two metal atoms using its two flexible arms to generate an infinite 1D hinged chain structure [Fig. 4(b)] and ligand **3** has a

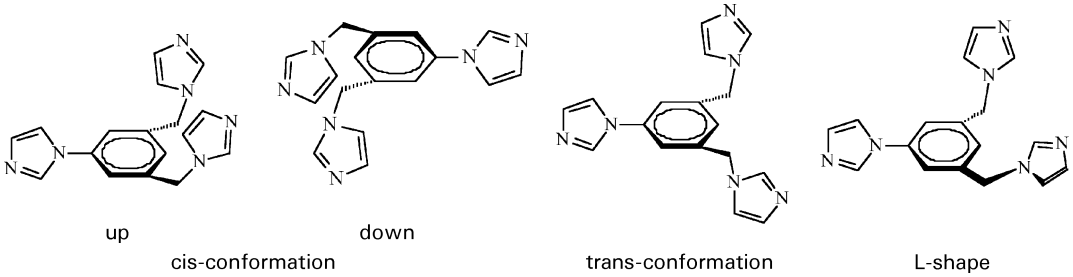

Scheme 2

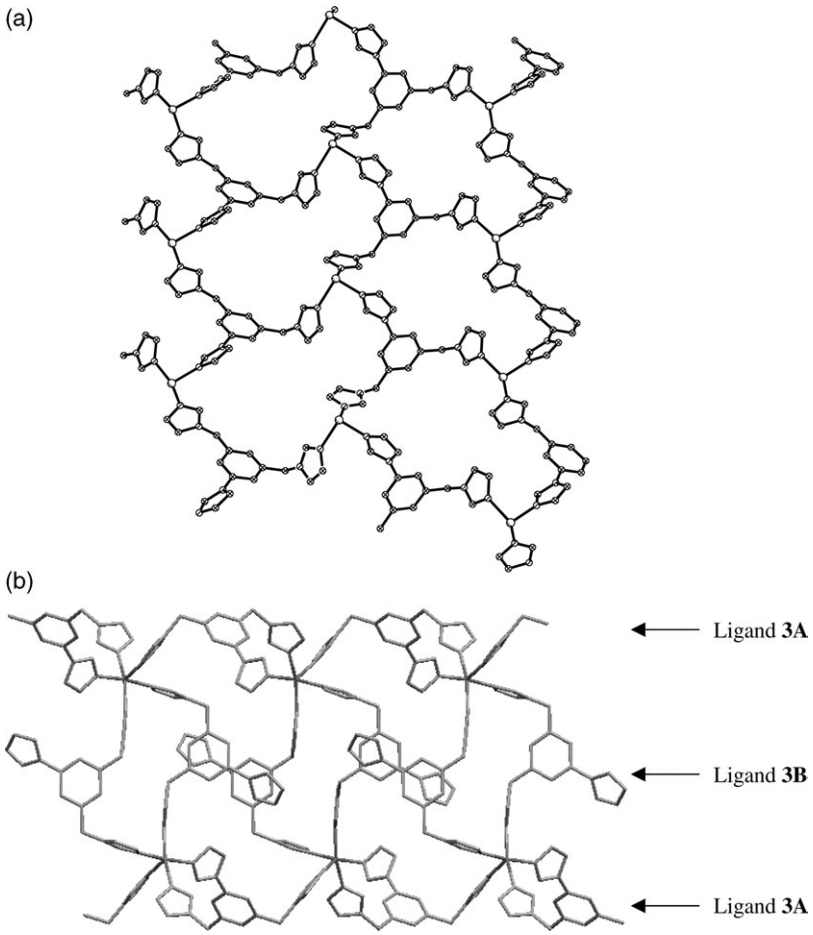

Fig. 2 (a) 2D honeycomb network in **4** formed by the coordination of the three-connecting ligands **3A** and the copper(II) atoms with the ligand **3B**; perchlorate anions, lattice water molecules and hydrogen atoms omitted for clarity. (b) Side view of the 2D network of **4** with the perchlorate anions, lattice water molecules and hydrogen atoms omitted for clarity.

cis conformation (Scheme 2). For ligand **3**, the three imidazolyl rings are inclined to the phenyl ring with angles of 85.1°, 93.8° and 142.2°, respectively. Intrachain metal-metal distances in complex **5** are 12.87 Å. It is noteworthy that ligand **3** in complex **5** has only two of its three imidazole groups coordinated with metal atoms; the third one is uncoordinated, which is similar to the ligand **3B** in complex **4**. The two benzene rings from two opposing **3** ligands in the $Cu_2(\mathbf{3})_2$ macrocyclic ring adopt a face-to-face conformation and are strictly parallel to each other with a centroid-centroid distance of 5.32 Å. In addition, in the dianion $Cu(mal)_2^{2-}$, each copper(II) center coordinates to four O atoms from two malonates with O–Cu–O bond angles ranging from 85.48(9)° to 180.0° and Cu–O band distances of 1.912(2) and 1.927(2) Å, respectively. It is obvious that a similar coordination geometry is found for Cu1 and Cu2; the Cu2 atom is in the plane composed of O1, O3, O1A, O3A without deviation. $Cu(mal)_2^{2-}$ and five uncoordinated water molecules are joined together by O–H···O hydrogen bonds with O···O distances in the range of 2.732(4)–2.903(3) Å to form an interesting 2D hydrogen-bonded structure in the *ab* plane [Fig. 4(c)]. Such 2D anionic layers are located in the voids formed between two adjacent cationic chains as exhibited in Fig. 5. Infinite 1D hinged chains and 2D hydrogen-bonded layers are repeated and joined by C–H···O hydrogen bonds with C···O distances in the range of 3.224(4)–3.437(4) Å to give a 3D structure for complex **5** as illustrated in Fig. S2 (Table S1; see the ESI). A previously reported malonato-bridged copper(II) complex, $\{(H_2bpe)[Cu(mal)_2]\}_n \cdot 4nH_2O$ [bpe = 1,2-bis(4-pyridyl)ethylene], consists of anionic malonato-bridged copper(II) chains that are connected through hydrogen bonds involving malonato oxygen atoms, uncoordinated water molecules and H_2bpe^{2+} cations.[20]

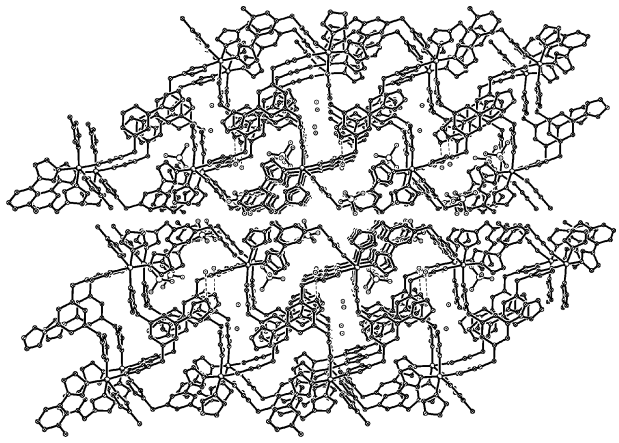

Fig. 3 Crystal packing diagram for complex **4**.

$[Cd(3)_2](NO_3)_2 \cdot H_2O$ (6). In addition to the synthesis of Cu(II) complexes with a coordination number of four or five, reactions of **3** with Cd(II) salts (cadmium is generally six-coordinated) were also carried out and complexes **6** and **7** were obtained. The polymeric structure of **6** was confirmed by X-ray single crystal structure analysis. The complex crystallizes in triclinic space group *P*-1 and Fig. 6 shows the asymmetric unit of **6** with atom numbering scheme. Each cadmium(II) atom is coordinated by six imidazole N atoms derived from six different **3** ligands. The coordination geometry of the Cd(II) center is a slightly distorted octahedral with coordination angles

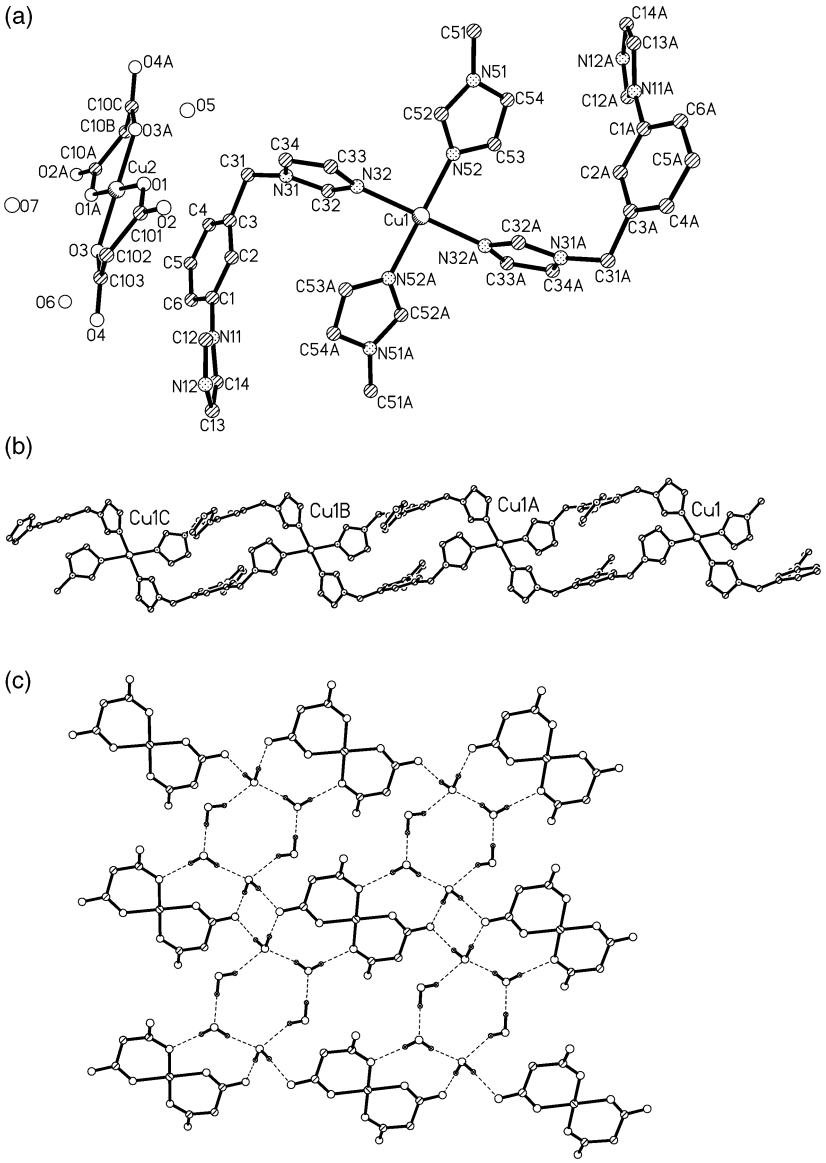

Fig. 4 (a) Coordination environment around the copper(II) atoms in **5** with the hydrogen atoms omitted for clarity. (b) 1D hinged chain structure in **5** with $Cu(mal)_2^{2-}$, lattice water molecules and hydrogen atoms omitted for clarity. (c) 2D hydrogen-bonded structure in the *ab* plane in **5** obtained by the connectivity of $Cu(mal)_2^{2-}$ and water molecules through O–H···O hydrogen bonds.

(N–Cd–N) ranging from 83.89(17)° to 178.36(17)° and the Cd–N bond lengths varying from 2.298(5) to 2.379(5) Å (Table 2). Each ligand **3** in turn connects three Cd(II) atoms, which form a triangle with edge lengths (Cd···Cd) of 12.99 Å (*e.g.*, Cd1B···Cd1C), 9.85 Å (*e.g.*, Cd1B···Cd1G) and 8.77 Å (*e.g.*, Cd1C···Cd1G), respectively. Such a coordination mode makes the compound a 2D network with honeycomb structure [Fig. 7(a)], and a schematic drawing is shown in Fig. 7(b). It is obvious that all **3** ligands in the network have cis conformation with alternating up and down orientations (Scheme 2). The distance between the two benzene ring planes of the up and down orientations is 10.83 Å and they are parallel each other.

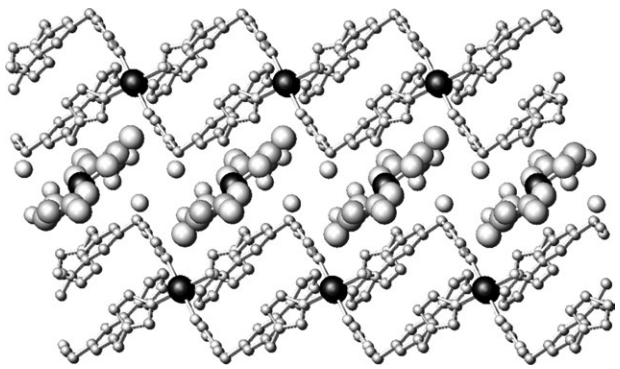

Fig. 5 1D polymeric chain representation of complex **5** with $Cu(mal)_2^{2-}$ and water molecules located in the voids formed between two adjacent cationic chains shown; hydrogen atoms are omitted for clarity.

The crystal packing diagram of complex **6** is illustrated in Fig. 8. The nitrate anions and the lattice water molecules are located in the voids formed between two adjacent cationic layers. As shown in Fig. S3 (ESI), the nitrate anions and the lattice water molecules are held there by C–H···O hydrogen bonds as tabulated in Table S1 (ESI).

$[Cd(3)(OAc)_2]\cdot 6H_2O$ (7). The crystallographic study provides direct evidence for the structure of **7**. As listed in Table 1, the complex crystallizes in triclinic space group *P*-1 and Fig. 9 shows the asymmetric unit of **7** with atom numbering scheme. Each cadmium(II) atom is coordinated with three N atoms of the imidazole unit from three different **3** ligands with N–Cd–N bond angles varying from 88.45(6)° to 169.61(6)° and Cd–N bond distances ranging from 2.278(2) to 2.320(2) Å (Table 2). The Cd1 atom locates within the plane formed by N12, N32,

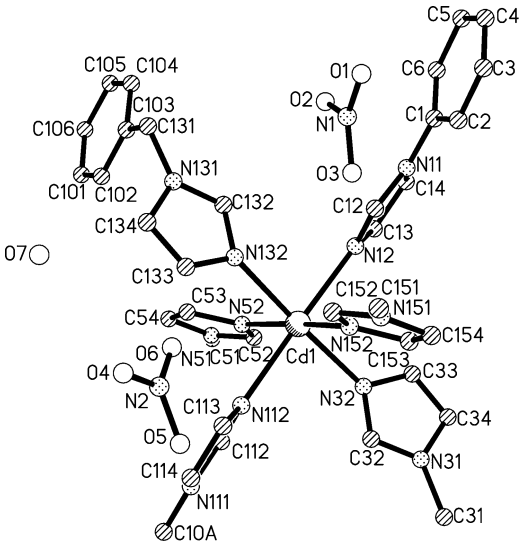

Fig. 6 Coordination environment around the cadmium(II) atom in **6** with the hydrogen atoms omitted for clarity.

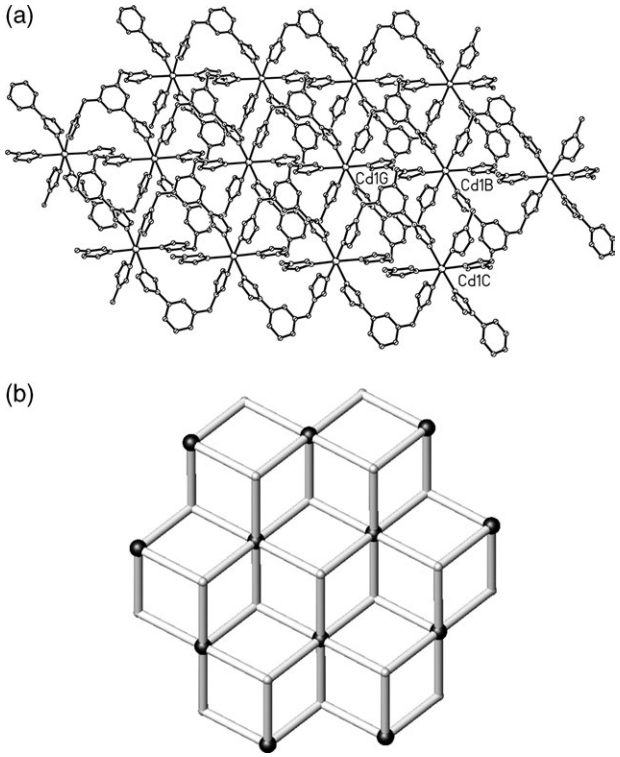

Fig. 7 (a) 2D honeycomb network in **6**; nitrate anions, lattice water molecules and hydrogen atoms are omitted for clarity. (b) Schematic drawing of the two-dimensional network of **6**, in which the ligands are represented by three spokes radiating from a point and the cadmium centers by black balls.

N52 atoms without deviation. Three additional positions are occupied by three O atoms from two different acetate anions with O–Cd–O bond angles of 143.58(6)°, 96.04(5)° and 52.71(5)° and Cd–O bond distances of 2.302(2), 2.394(2) and 2.500(2) Å, respectively (Table 2). Therefore the coordination environment of the cadmium(II) atom is N_3O_3, which is different from that in **6**. In turn, each **3** ligand links three metal atoms to form a triangle with edge lengths (Cd···Cd) of 12.12, 11.24 and 13.48 Å, respectively. The three imidazolyl rings are inclined to the phenyl ring with angles of 77.2°, 107.9° and 162.2°. As shown in Fig. 10, such a coordination mode generates an infinite 2D grid network structure based on (6,3) nets and the **3** ligand has a trans conformation (Scheme 2), which is different from that in **4**, **5**, and **6**.

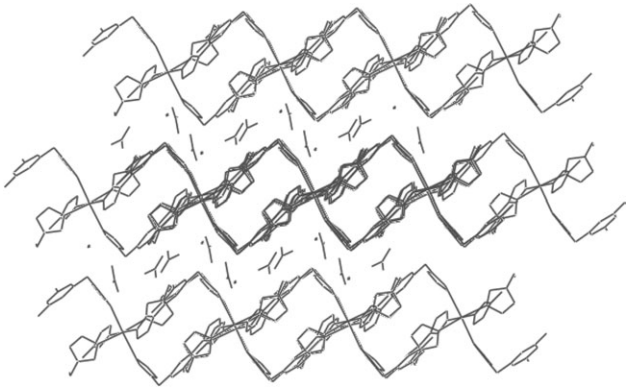

Fig. 8 Crystal packing diagram for complex **6**.

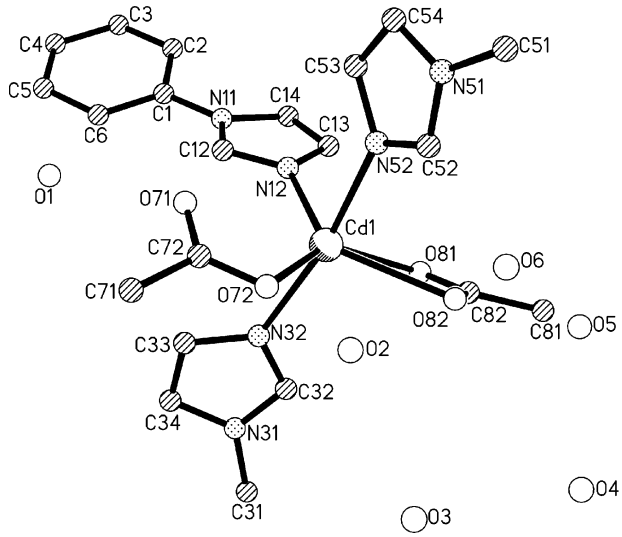

Fig. 9 Coordination environment around the cadmium(II) atom in **7** with the hydrogen atoms omitted for clarity.

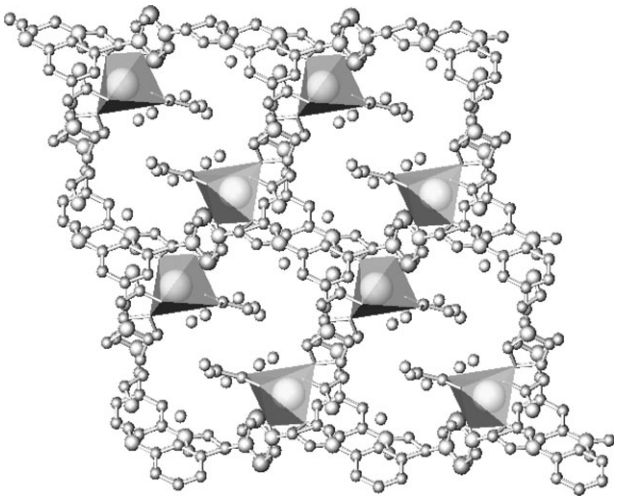

Fig. 10 2D polymeric grid network of complex **7**.

The crystal packing diagram of complex **7** is illustrated in Fig. 11. The 2D sheets are further connected by O–H···O hydrogen bonds to give a 3D structure as shown in Fig. S4(a) (ESI). It is noteworthy that the connectivity of the water molecules with the acetate ligands generates an interesting 3D framework [Fig. S4(b), ESI]; the hydrogen bonding data are listed in detail in Table S1 (ESI). There are large open channels in complex **7**, which are occupied by water molecules held there by C–H···O and O–H···O hydrogen bonds (Table S1).

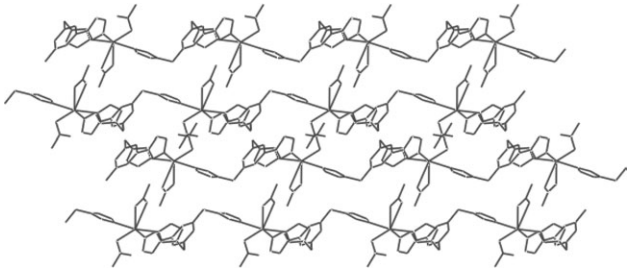

Fig. 11 Crystal packing diagram for complex **7** with the lattice water molecules and hydrogen atoms omitted for clarity.

Comparison of structures. The results showed that the nature of the metal ion has an important influence on the structures of the MOFs with ligand **3**. Due to the different coordination geometry requirements of the metal ions, coordination compounds **4**, **5** and **6**, **7** have different structures, in which ligand **3B** in **4** and ligand **3** in **5** both have only two of the three imidazole groups coordinated with metal atoms while the third one keeps free of coordination. In addition to the role of the metal atoms, counter anions with different shapes, coordination and bridging abilities also have a remarkable impact on the structure of the MOFs; for example, complexes **6** and **7** with nitrate and acetate anions have different structures, though Cd(II) in **6** and **7** has the same six-coordination. It is noteworthy that in complex **7**, ligand **3** has a trans conformation and leads to a 2D grid network structure.

The present study also shows that the reactions of flexible organic ligands with various metal salts can afford a variety of fascinating self-assembled polymeric frameworks. The difference between ligands **3** and **1** is that the former is more flexible than the latter. Flexible ligand **3** can adjust its conformation to fit with the geometrical needs of metal ions. For example, in complex **4**, ligand **3A** adopts a cis conformation to give a 2D honeycomb network, while in a previously reported complex $[Cu(\mathbf{1})_2(H_2O)_2](ClO_4)_2$[12] obtained by reaction of $Cu(ClO_4)_2 \cdot 6H_2O$ with ligand **1**, each ligand **1** coordinates to two copper(II) atoms as a bidentate ligand rather than as a tridentate one. Such a difference is caused by the introduction of methylene groups between the imidazole and central benzene groups in **3**. Previous studies showed that 1D hinged chain and 2D network structures were obtained by reactions of another flexible tripodal ligand **2** with $MnSO_4 \cdot H_2O$ and $Mn(ClO_4)_2 \cdot 6H_2O$,[12] which are similar with complexes **5** and **6**, respectively. The results show that the nature of the organic ligand has a great impact on the structures of the assembly products.

Anion-exchange properties of complex 6

As revealed by the crystal structure of **6**, the anions are located within the open structure between the cationic layers through hydrogen bonds (Fig. 8). Since complex **6** is insoluble in common solvents, this cationic layered compound is expected to display anion-exchange properties. Excess $NaClO_4$ was added to a well-ground powder of complex **6** suspended in water at room temperature. The mixture was stirred for 24 h to allow anion exchange, then it was filtered and washed with water several times. The FT-IR spectra of the exchanged solid and the original **6** are shown in Fig. 12 as traces b and a, respectively. Intense bands at $\nu = 1112$ to 1091 cm^{-1} appeared, which originate from the ClO_4^- ion, while the intense bands from 1384 to 1356 cm^{-1} of the NO_3^- ion disappeared in the spectrum of the exchanged solid. The result of elemental analysis also suggests complete anion exchange (see Experimental). The anion-exchange reactions were also monitored by X-ray powder diffraction (XPD) techniques (Fig. S6 in ESI). The similar XPD patterns observed for the exchanged product suggest that the solid state structure is retained. To investigate

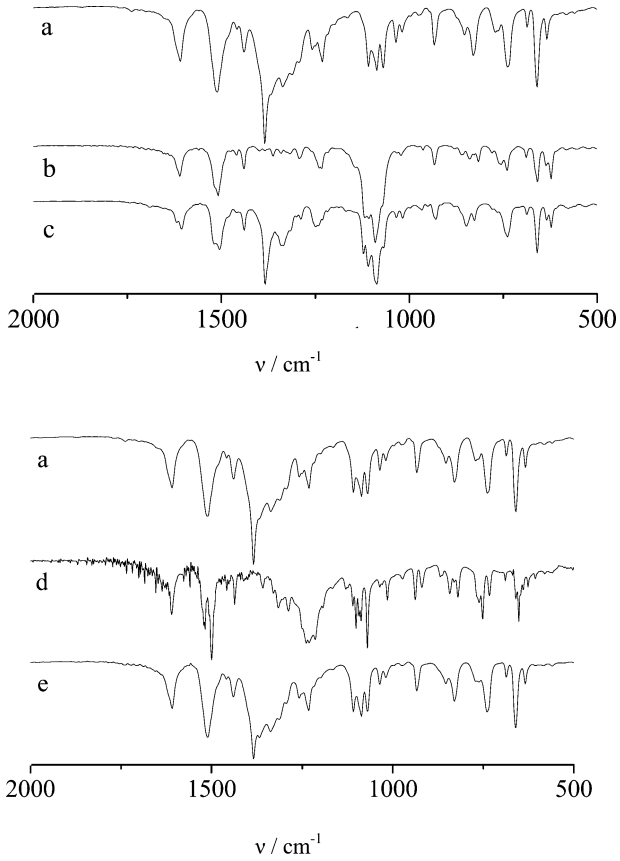

Fig. 12 FT-IR spectra of (a) complex **6**, (b) complex **6** treated with an aqueous solution of $NaClO_4$, (c) complex **6** treated with an aqueous solution of $NaClO_4$ and then with $NaNO_3$, (d) complex **6** treated with an aqueous solution of $NaNO_2$, (e) complex **6** treated with an aqueous solution of $NaNO_2$ and then with $NaNO_3$.

the reversibility of such anion-exchange processes in more detail, the exchanged solid was suspended in an aqueous solution of $NaNO_3$ with stirring to allow anion exchange again. It is interesting that both the ClO_4^- and NO_3^- bands appeared in the FT-IR spectrum of the obtained solid (trace c in Fig. 12). The result of elemental analysis suggests *ca.* 50% exchange of ClO_4^- by NO_3^-, namely the exchange product would be $[Cd(\mathbf{3})_2](ClO_4)(NO_3) \cdot H_2O$ (see Experimental). The anion exchange was also carried out between complex **6** and $NaNO_2$. The FT-IR spectrum of the exchanged solid is shown as trace d in Fig. 12. Intense bands at $\nu = 1335$ to 1250 cm^{-1}, which originate from the NO_2^- ion, appeared while the intense bands from 1384 to 1356 cm^{-1} of the NO_3^- ion disappeared in the spectrum of the exchanged solid, implying complete anion exchange. The exchanged solid was again suspended in an aqueous solution of $NaNO_3$ with stirring to allow anion exchange. The NO_2^- bands disappeared and the NO_3^- bands appeared in the FT-IR spectrum of the obtained solid (trace e in Fig. 12), which is almost the same as the spectrum of the original material **6** (trace a in Fig. 12). The XPD pattern of exchanged product closely resembles the experimental one of **6** [*cf.*Fig. S6(e) with Fig. S6(a) in the ESI]. The FT-IR and elemental analysis confirm the reversible anion exchange between NO_3^- and NO_2^- anions.

In complex **6**, the nitrate anions could be exchanged by the perchlorate anions, however, the perchlorate anions could only be partially exchanged by the nitrate anions, probably due to the different environments around the two ClO_4^- in $[Cd(\mathbf{3})_2](ClO_4)_2 \cdot H_2O$. As discussed by Yip *et al.*,[11b] the exchange of $[Cd(\mathbf{3})_2](NO_3)_2 \cdot H_2O$ by ClO_4^- is favored since the hydration energy (ΔG_h) of NO_3^- (-300 kJ mol^{-1}) is higher than that of ClO_4^- (-205 kJ mol^{-1}). On the other hand, reversible anion exchange between complexes $[Cd(\mathbf{3})_2](NO_3)_2 \cdot H_2O$

and $[Cd(\mathbf{3})_2](NO_2)_2 \cdot H_2O$ may be due to the comparability of the nitrate anions and the nitrite anions.

Acknowledgements

The authors are grateful to the National Natural Science Foundation of China (Grant No. 20231020) for financial support of this work.

References

1 See, for example: *Comprehensive Supramolecular Chemistry*, eds. J. L. Atwood, J. E. D. Davies, D. D. MacNicol, F. Vögtle and J. M. Lehn, Pergamon, Oxford, 1996, vol. **9**, ch. 1–8.
2 G. B. Gardner, D. Ventakaraman, J. S. Moore and S. Lee, *Nature (London)*, 1995, **374**, 792.
3 (*a*) S. R. Batten, B. F. Hoskins and R. Robson, *J. Am. Chem. Soc.*, 1995, **117**, 5385; (*b*) B. F. Abrahams, S. R. Batten, H. Hamit, B. F. Hoskins and R. Robson, *Angew. Chem., Int. Ed. Engl.*, 1996, **35**, 1690; (*c*) B. F. Abrahams, S. R. Batten, M. J. Grannas, H. Hamit, B. F. Hoskins and R. Robson, *Angew. Chem., Int. Ed.*, 1999, **38**, 1475; (*d*) S. R. Batten, B. F. Hoskins, B. Moubaraki, K. S. Murray and R. Robson, *Chem. Commun.*, 2000, 1095.
4 B. L. Chen, M. Eddaoudi, S. T. Hyde, M. O'Keeffe and O. M. Yaghi, *Science*, 2001, **291**, 1021.
5 M. Fujita, S. Nagao and K. Ogura, *J. Am. Chem. Soc.*, 1995, **117**, 1649.
6 C.-Y. Su, Y.-P. Cai, C.-L. Chen, F. Lissner, B.-S. Kang and W. Kaim, *Angew. Chem., Int. Ed.*, 2002, **41**, 3371.
7 For examples, see: (*a*) H.-K. Liu, W.-Y. Sun, W.-X. Tang, T. Yamamoto and N. Ueyama, *Inorg. Chem.*, 1999, **38**, 6313; (*b*) H.-K. Liu, W.-Y. Sun, D.-J. Ma, K.-B. Yu and W.-X. Tang, *Chem. Commun.*, 2000, 591; (*c*) W.-Y. Sun, J. Xie, T. Okamura, C.-K. Huang and N. Ueyama, *Chem. Commun.*, 2000, 1429; (*d*) W.-Y. Sun, J. Fan, T. Okamura, J. Xie, K.-B. Yu and N. Ueyama, *Chem.-Eur. J.*, 2001, **7**, 2557; (*e*) J. Fan, W.-Y. Sun, T. Okamura, J. Xie, W.-X. Tang and N. Ueyama, *New J. Chem.*, 2002, **26**, 199; (*f*) J. Fan, B. Sui, T. Okamura, W.-Y. Sun, W.-X. Tang and N. Ueyama, *J. Chem. Soc., Dalton Trans.*, 2002, 3868; (*g*) J. Fan, H. F. Zhu, T. Okamura, W.-Y. Sun, W.-X. Tang and N. Ueyama, *Inorg. Chem.*, 2003, **42**, 158; (*h*) S.-Y. Wan, Y.-Z. Li, T. Okamura, J. Fan, W.-Y. Sun and N. Ueyama, *Eur. J. Inorg. Chem.*, 2003, 3783.
8 (*a*) S. I. Noro, S. Kitagawa, M. Yamashita and T. Wada, *Chem. Commun.*, 2002, 222; (*b*) M. Munakata, L. P. Wu and T. Kuroda-Sowa, *Bull. Chem. Soc. Jpn.*, 1997, **70**, 1727.
9 (*a*) R. H. Groeneman, L. R. MacGilliray and J. L. Atwood, *Chem. Commun.*, 1998, 2735; (*b*) Y. Cui, O. R. Evans, H. L. Ngo, P. S. White and W. B. Lin, *Angew. Chem., Int. Ed.*, 2002, **41**, 7; (*c*) D. M. L. Goodgame, D. A. Grachvogel and D. J. Williams, *Angew. Chem., Int. Ed.*, 1999, **38**, 153.
10 (*a*) C. V. K. Sharma and M. J. Zaworotko, *Chem. Commun.*, 1996, 2655; (*b*) D. L. Long, A. J. Blake, N. R. Champness, C. Wilson and M. Schröder, *Chem.-Eur. J.*, 2002, **9**, 2026.
11 (*a*) O. M. Yaghi and H. L. Li, *J. Am. Chem. Soc.*, 1995, **117**, 10 401; (*b*) S. Muthu, J. H. K. Yip and J. J. Vittal, *J. Chem. Soc., Dalton Trans.*, 2002, 4561.
12 J. Fan, L. Gan, H. Kawaguchi, W.-Y. Sun, K.-B. Yu and W.-X. Tang, *Chem.-Eur. J.*, 2003, **9**, 3965.
13 J. S. Fleming, K. L. V. Mann, C.-A. Carraz, E. Psillakis, J. C. Jeffery, J. A. McCleverty and M. D. Ward, *Angew. Chem., Int. Ed.*, 1998, **37**, 1279.
14 (*a*) P. N. W. Baxter, J.-M. Lehn, G. Baum and D. Fenske, *Chem.-Eur. J.*, 1999, **5**, 102; (*b*) P. N. W. Baxter, J.-M. Lehn, B. O. Kneisel, G. Baum and D. Fenske, *Chem.-Eur. J.*, 1999, **5**, 113; (*c*) D. T. Tran, P. Y. Zavalij and S. R. J. Oliver, *J. Am. Chem. Soc.*, 2002, **124**, 3966.
15 O. M. Yaghi, H. Li, C. Davis, D. Richardson and T. L. Groy, *Acc. Chem. Res.*, 1998, **31**, 474.
16 A. Altomare, M. C. Burla, M. Camalli, G. Cascarano, C. Giacovazzo, A. Guagliardi and G. Polidori, *J. Appl. Crystallogr.*, 1994, **27**, 435.
17 P. T. Beurskens, G. Admiraal, G. Beurskens, W. P. Bosman, R. de Gelder, R. Israel and J. M. M. Smits, *The DIRDIF-94 program system*, Crystallography Laboratory, University of Nijmegen, The Netherlands, 1994.
18 *teXsan: Crystal Structure Analysis Package*, Molecular Structure Corporation, The Woodlands, TX, USA, 1999.
19 G. R. Desiraju, *Acc. Chem. Res.*, 1996, **29**, 441.
20 F. S. Delgado, J. Sanchiz, C. Ruiz-Pérez, F. Lloret and M. Julve, *Inorg. Chem.*, 2003, **42**, 5938.